Vibration-based Rotorcraft Gearbox Monitoring Under Varying Operating Conditions

First Cristobal Ruiz-Carcel[1], Andrew Starr[1], James R. Ottewill[2], and Victor H. Jaramillo[2,3]

[1]*Cranfield University, Cranfield, Bedfordshire MK430AL, United Kingdom*
c.ruizcarcel@cranfield.ac.uk
a.starr@cranfield.ac.uk

[2] *ABB Corporate Research Center, Ul. Starowiślna 13A, 31-038 Kraków, Poland*
james.ottewill@pl.abb.com

[3] *currently at: Universidad EIA, Mechatronics Engineering Department, 055428 Envigado, Colombia*
victor.jaramillo92@eia.edu.co

ABSTRACT

Modern rotorcrafts rely on Health and Usage Monitoring Systems (HUMS) to enhance their availability, reliability and safety. The complexity of the transmission system of new helicopter designs such as the Airbus Racer provides additional challenges for HUMS. The work presented here demonstrates a vibration-based monitoring approach for the lateral gearboxes of the racer. This approach relies on the statistical analysis of different condition indicators (CIs) extracted from vibration signals under different operating regimes to define a baseline for these CIs during normal operation. This permits the normalization of CIs from newly acquired signals with respect to the expected baseline value, facilitating the detection of anomalies in the signal characteristics for a variety of operating regimes. The monitoring capabilities of the proposed approach are tested using experimental data where the vibration response to different mechanical malfunctions was artificially seeded in to the acquired signals.

1. INTRODUCTION

Power transmissions in rotorcrafts are exposed to extreme loads and sustained high levels of vibration. Typically, lightweight materials and designs are used to improve the performance of the aircraft. As a consequence many maintenance actions in helicopters are triggered by premature degradation due to fatigue in critical components (Samuel & Pines, 2005). Health and Usage Monitoring Systems (HUMS) use data collected from a number of sensors and different signal processing techniques to provide information about the health condition of the machine. This information is then used for maintenance scheduling, which reduces maintenance and operating costs by improving the availability, reliability and safety of the aircraft.

Vibration-based condition monitoring is probably the most common method for detection and diagnosis of mechanical faults in rotating machinery. HUMS systems typically rely on vibration signals in order to monitor the condition of the transmission system (Morgan, Berrigan, Lopez, & Prasad, 2017). Typically vibration-based monitoring techniques rely on the analysis of key signal features that are particularly sensitive to different mechanical malfunctions. The baseline values for these features are obtained under healthy conditions, and values extracted from new observations are compared with this baseline in order to detect anomalies in the signal. However, different operating regimes will produce different vibration characteristics (McFadden, 1986). Consequently this direct comparison is only effective if all of the measurements were obtained under the same speed and loading conditions. In the case of the lateral gearboxes of the RACER, dynamic operation (speed and torque) is defined by the rotational speed and the blade pitch angle (aircraft speed and other dynamic effects are not considered here for simplicity).

The problem of vibration-based condition monitoring under variable operating conditions has been approached for other applications in the past using different techniques such as band pass filtered time-domain synchronous averaging (TSA) and Hilbert transform (McFadden, 1986), time-frequency mapping (Baydar & Ball, 2001), bispectral analysis (Parker Jr. et al., 2000) or motion residuals (Zhan, Makis, & Jardine, 2006). More recently, experimental case studies applied to mining machinery (Zimroz, Bartelmus, Barszcz, & Urbanek, 2014) or wind turbines (Bartelmus &

Zimroz, 2009) have demonstrated that the correlation between load and selected signal features can be used to monitor the condition of the machine.

New rotorcraft designs provide additional challenges for HUMS. In particular, the new Airbus RACER rotorcraft design combines a traditional horizontally mounted rotor with additional vertically mounted rotors on its wings for improved propulsion while maintaining vertical take-off and landing capabilities. These lateral rotors are powered from the main gearbox using an additional shaft at each side of the aircraft (see Figure 1). An additional lateral gearbox at the end of each shaft is required to accommodate the angle between the transmission and the propeller shafts. The Clean Sky 2 funded project "iGear" (involving GE Avio Aero, Active Space Technologies and Cranfield University) aims to develop a multi sensor health monitoring system for the lateral gearboxes of the RACER.

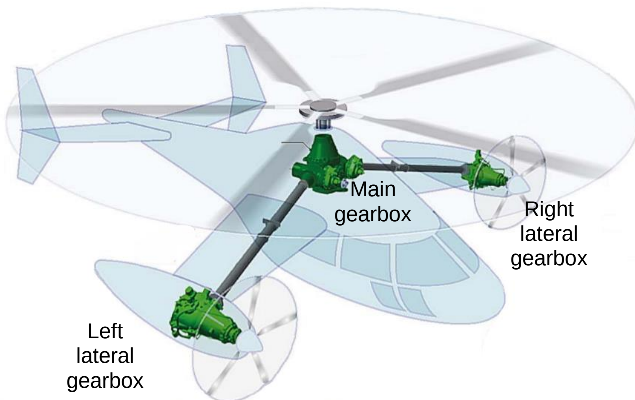

Figure 1: Racer transmission layout

The objective of this investigation in particular is to test a conceptual approach to analyse the vibration signals of rotating machinery under varying operating conditions for its future application in rotorcrafts. This approach makes use of operating condition measurements to generate a map of each individual condition indicator (CI) extracted from vibration signals within a defined range of operating regimes. This map is used to define the limit values at any operating condition for each CI individually, allowing a fair comparison between CIs from newly acquired measurements and the expected CI value for that particular operating regime. This method provides a simple and computationally efficient method to cope with varying operating conditions, while facilitating the traceability in case of fault detection. This approach was tested using experimental data to generate baseline maps for a number of selected CIs. Subsequently, the acquired vibration signals were contaminated to simulate the effect of mechanical faults. The comparison of CIs from contaminated signals and the baseline values mapped under normal operation was used to assess the monitoring capabilities of the algorithm.

2. METHODOLOGY

2.1. CI mapping approach

The CI baseline maps are based on statistical analysis of the CI values for a range of operating conditions. In order to reduce the effect of outliers and study data points with similar characteristics, the operating points considered need to be pre-processed before the CI values can be mapped. The whole mapping procedure consists of four steps: steadiness check, operating regimes clustering, statistical analysis at each cluster and finally curve fitting to generate the map. These steps are summarised below.

1) Steadiness check: Although the condition monitoring system should work for different operating regimes (speed and torque), rapid changes occurring during the transition from one operating point to another may have non-linear effects on the system dynamics. A short-term vibration response with significantly different characteristics may be produced by these transients, making the identification of fault signatures more difficult and hence leading to missed detections or false alarms.

   Due to the short duration of these transients, the proposed approach detects them in the first place by evaluating the evolution of the operating condition measurements and dismissing those measurements which are deemed not steady. Hence the first task in the data analysis is to use a moving window which includes a given number of previous measurements at each point considered, and check that the measurement deviations are contained within a certain margin.

2) Operating regimes clustering: In this second step the operating condition measurements are grouped in clusters with similar characteristics. This procedure allows the analysis of signal features in a dataset acquired under similar conditions while accounting for small variations in the measurements. The evolving clustering method (ECM) is an unsupervised clustering technique based on a maximum distance criterion. Basically it generates a set of clusters (defined by a centre position and a radius) so that any sample considered is located within a maximum Euclidean distance from a cluster centre. The mathematical procedure was described in detail in (Kasabov & Song, 2002).

3) Statistical analysis of clustered data: The organization of the operating condition measurements in clusters allows the study of the statistical distribution of the CIs extracted from vibration signals located in the same cluster. The features in each cluster would have been acquired under very similar operating conditions and hence

should have similar properties in the absence of faults. In the proposed approach the probability density function (PDF) of each CI is estimated in each cluster considering all of the samples assigned to it. Although the variations in these CIs are random in principle and hence should follow a normal distribution, kernel density estimators were used to obtain a smooth and accurate representation of the actual PDF. This detailed characterization of the statistical distribution was used to stablish an upper limit at each cluster centre for each one of the CIs considered for a given confidence bound.

4) Condition indicator mapping: The upper control limits at each cluster centre together with the cluster centres location were used to generate a map of the maximum allowable value for each CI at any possible operating condition. This mathematical model is generated by fitting a surface through these points. The corresponding upper limit of a CI acquired at a given operating condition can be obtained interpolating the value from this map, even if such point was acquired under operating conditions not tested before.

2.2. Condition monitoring using normalised CIs

Once the baseline maps are defined for each CI within the considered operating range, any CI from newly acquired vibration measurement at a given operating point can be compared with its corresponding value in the baseline map. This comparison allows a normalization of the new CIs with respect to the baseline value, giving a value equal or lower than one if the value of the CI is lower than the upper limit for that particular operating point, and higher than one otherwise.

This approach allows an automatic adaptation of the upper limit according to the operation, minimising the effect of the operating conditions on the CI value. In addition, it normalises all of the CIs considered to the same scale, facilitating the comparison between different CIs and its combination in future stages of the project.

2.3. Injection of faulty signals in healthy vibration data

In order to assess the monitoring performance of the proposed methodology it is necessary to use operation and vibration measurements from a system working under changing operational conditions in the presence of faults. For safety reasons it was not possible to introduce mechanical faults in the test rig (described in 3) whilst ensuring the mechanical integrity of all its components. For that reason the vibration signature of different mechanical faults was simulated and then seeded in the healthy vibration signals acquired, following the same procedure as in (Ruiz-Cárcel, Jaramillo, Mba, Ottewill, & Cao, 2016) .

The effect of the forces generated by a mechanical fault can be represented as a residual load $\Delta F(t)$ which acts on the undamaged system adding this new force to the forces already existing. Consequently, the motion observed in the damaged system $u(t)$ is the result of the addition of the motion caused by the excitation forces in the undamaged system $u_0(t)$ and the motion caused by the virtual damage forces $\Delta u(t)$. The problem can be represented in a simplified manner as a one degree of freedom system where a mass m is connected to the foundation by an elastic element with stiffness K and a viscous damper with damping D which, during normal operation is subjected to a force $F_0(t)$. The motion $u(t)$ of the damaged system can be obtained by solving the equation:

$$m\ddot{u}(t) + c\ddot{u}(t) + ku(t) = F_0(t) + \Delta F(t) \qquad (1)$$

As $u_0(t)$ is the measured signal, the virtual damage motion $\Delta u(t)$ can be estimated for a given damage force $\Delta F(t)$ as:

$$\Delta u(t) = conv(\Delta F(t), h(t)) \qquad (2)$$

where $h(t)$ is the impulse response function of the system. By adding this virtual motion (or the corresponding derivatives) to the measured undamaged signal it is possible to contaminate the original signal with the fault signature defined by $\Delta F(t)$. These artificially seeded faulty signals were used to test the capabilities of the algorithm under different faulty scenarios.

3. EXPERIMENTAL SET UP

The monitoring capabilities of the proposed approach were tested on a laboratory scale compressor rig (Figure 2). This rig is designed to be able to function over a wide range of operating conditions through the control of the motor rotational speed and the position of the valve situated in the compressor outlet line. This configuration is comparable to the lateral gearbox dynamic operation defined by rotational speed and blade pitch angle.

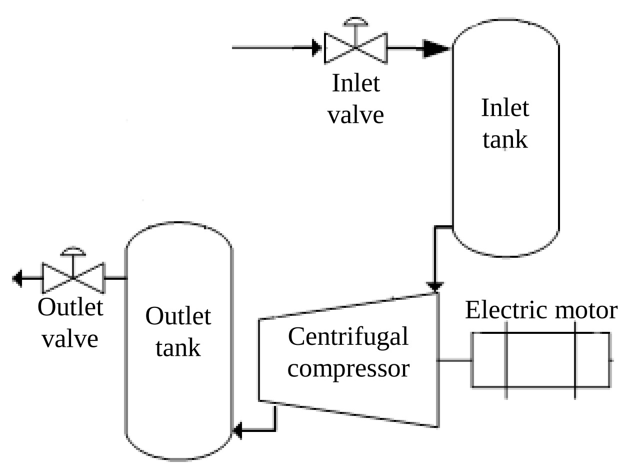

Figure 2: Schematic of the compressor rig

The set point of the motor speed and the outlet valve position were varied during the tests to different pre-set values to capture vibration data at different operating regimes. Speed and valve position measurements were acquired at 0.5 Hz, while vibration was acquired continuously using a SKF CMSS2110 (frequency range 0.8Hz-10kHz) accelerometer installed horizontally on the outer case of the motor drive-side bearing (see figure 3). This signal was digitised at 5120 Hz using a NI 9234 data acquisition card.

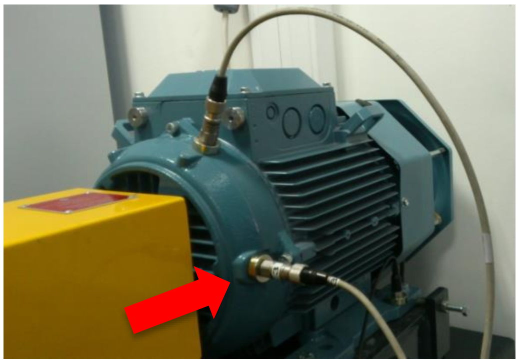

Figure 3: Sensor location detail

4. RESULTS AND DISCUSSION

4.1. Data sets analysed

A data set of 9662 s of duration was used to define the baseline maps. Four different set point values of motor speed (1000, 2000, 3000 and 4000 rpm) were combined with four outlet valve positions (40, 60, 80 and 100%) throughout the test duration to acquire data at 16 different operating points. The vibration data streamed during the test duration was divided in sections of 2 s, so that each speed and valve position measurement has a corresponding vibration measurement attached. The vibration CIs extracted from each vibration signal section to validate the mapping concept were:

- RMS, Crest factor (CF) and Kurtosis (K) extracted from the time domain signal
- Amplitude of the peaks at the rotational speed (1X) and its second harmonic (2X) obtained from the signal in the frequency domain.

Once the approach was implemented and the maps were defined, a second dataset (with a duration of 2790 s) was used to assess the performance of the method. In this validation data set the speed and valve position set points were also varied during the test, but the valve positions were different to those used in the training data set. Due to the lack of data acquired in presence of faults, the signals acquired were contaminated with faulty signals as described in 2.3 simulating the effect of mechanical faults.

The first simulated fault injected to the validation data set was rotor unbalance, caused by the displacement of the rotor centre of mass away from its rotation centre. The centrifugal force generated $\Delta F(t)$ has an amplitude proportional to the rotor mass m_r, the eccentricity e and the square of the rotational speed ω (1X), and has a phase angle δ:

$$\Delta F(t)= \omega^2 m_r e \cdot sin(\omega t+ \delta). \quad (3)$$

In order to test the capabilities of the method for detecting gear faults, a faulty gear signal simulating gear tooth wear in a virtual pinion with 15 teeth was injected to the existing signal. The faulty tooth gear meshing was simplified as a series of impacts happening at the rotation frequency (1X). In both cases, the faults were introduced in different stages of severity (eccentricity and meshing force amplitude) to test the sensitivity of the method. Once the residual loads related to these faults are defined, the faulty vibration response was obtained solving Eq. (2), and then added to the original signal. The physical parameters in Eq. (2) were set to m=55 kg, K=5E9 N/m and C= 1000 N/sm, giving a natural frequency of 1517 Hz. The mass of the rotor in the eccentricity case was set to 25 kg. Figure 4 shows an example of the vibration response of this system to a series of impacts.

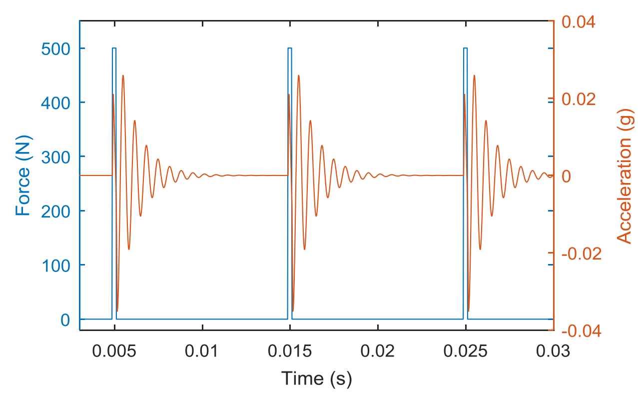

Figure 4: Signal response example

4.2. Condition indicator mapping and normalization

The first step in the approach described in 2.1 is a steadiness check to eliminate those data points considered not steady during the transition between operating points. The operating conditions in the data set used to generate the CI maps in absence of faults were analysed using a moving window of 4 data points. All measurements incurring in variations higher than 2 rpm in speed or 2 % in valve position were dismissed for further steps of the analysis. Figure 5 shows the results obtained from this analysis, where 186 samples were labelled as non-steady and not considered for the clustering process. The same procedure was applied to the operating conditions of the second data set used for validation.

The second step to produce the CI maps is the clustering of all the steady operating points observed. In first place the speed and valve position measurements in the training data set were normalised to a range of 0 to 1 and steady data samples were clustered using the ECM with a maximum

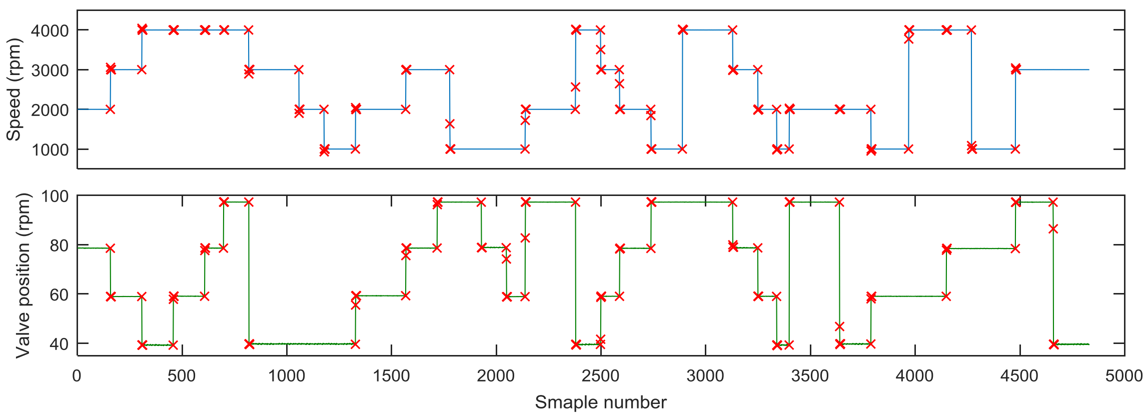

Figure 5: Steadiness analysis

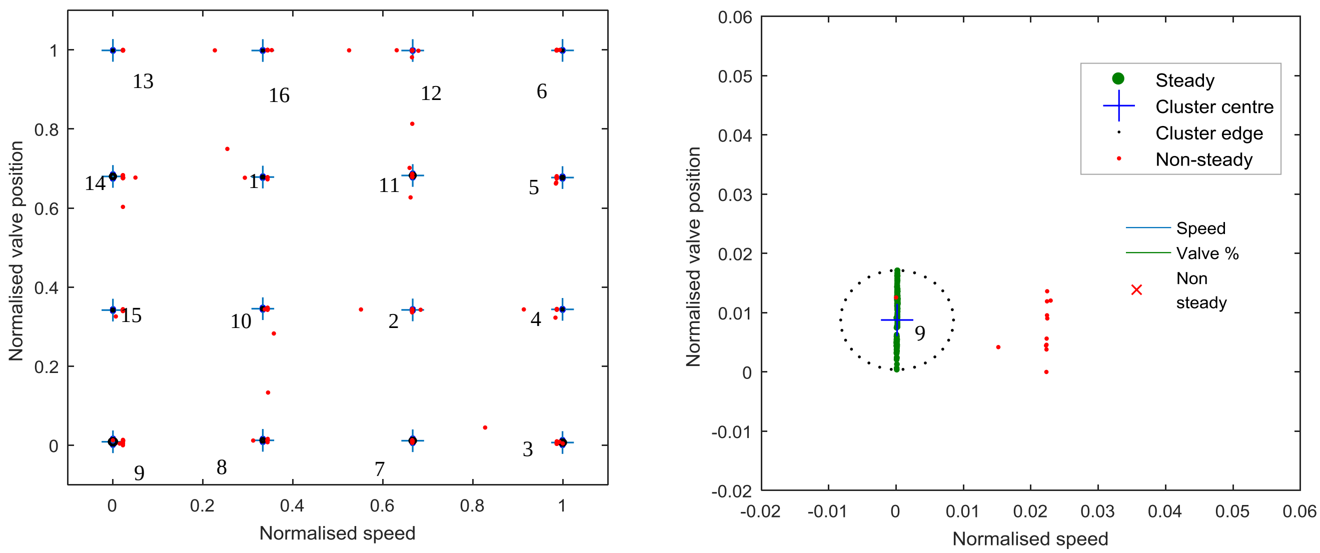

Figure 6: Clustered data (left) and cluster detail (right)

cluster diameter of 0.02. Figure 6 shows the clusters obtained (16 in this case), each one containing between 198 and 468 samples. The cluster detail on the right side of the figure shows how all of the steady samples around a cluster centre are contained within the cluster edge.

The statistical properties for each CI were studied individually, obtaining the corresponding PDF at each cluster. The cumulative probability was used to determine the upper limit at each cluster for a probability of 90%. Figure 7 shows an example of the cumulative PDFs of the 1X peak amplitude feature obtained for the 16 corresponding clusters. These PDFs provided the information necessary to set the upper limit value at each cluster location with a confidence bound of 90 %. The CI values obtained and the location of the clusters were used to generate a 3D map (cubic interpolation) where the upper limit of the CI can be interpolated for any operating condition (see Figure 8). Using the same procedure, the maps of the other CIs were also obtained. With these maps the values of the CIs extracted from the signals can be normalised to the upper limit value, minimising the influence of the operating conditions on the value of the CI.

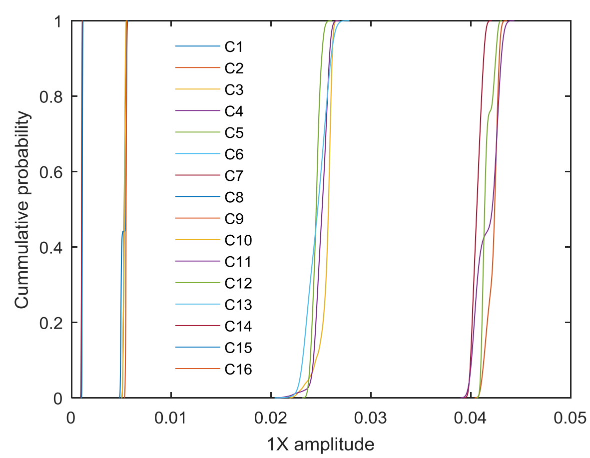

Figure 7: 1X amplitude cumulative probability at each cluster

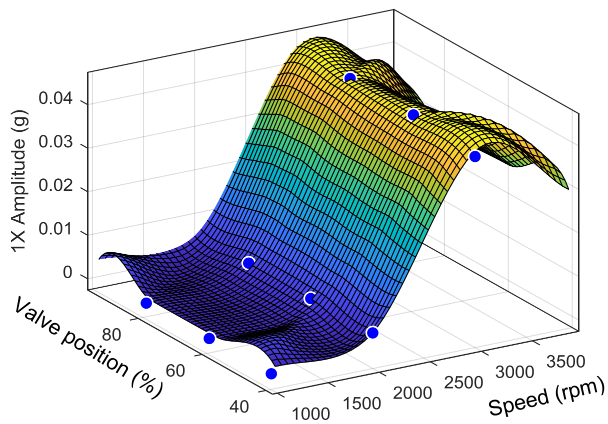

Figure 8: 1X peak amplitude map

The results of this normalization procedure applied to the validation data set can be seen in Figure 9. This data set contains 12 different operating points not tested in the training dataset, as the valve positions tested in this case were 50, 70 and 100%. As it may be observed from Figure 9, the raw CIs extracted have two main problems. The first problem is the difference in magnitude (note the logarithmic scale in the y axis) inherent to the nature of each indicator, which makes the comparison and correlation of different CIs more difficult. The second and main problem is the dependency of the value of each indicator and the operating conditions, which is also obvious from the shape of the 3D map in Figure 8. By normalising the CIs at each observation to its corresponding baseline value this dependency is minimised. The percentages of observations found over the baseline value (normalised value higher than 1) in the validation data set were 10.1 13.9 15.7 12.9 and 12.7% for the RMS, CF, K, 1X and 2X amplitudes respectively.

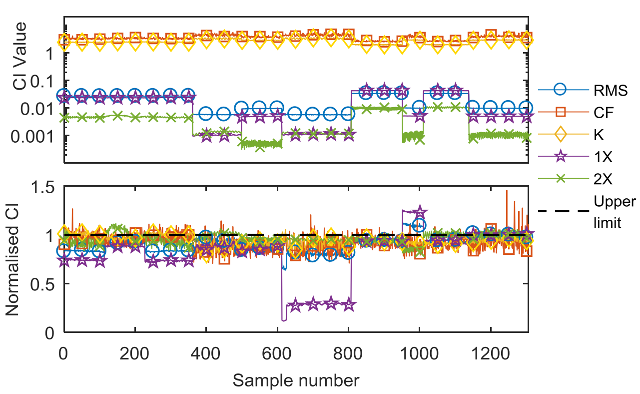

Figure 9: CI values before (top) and after (bottom) normalization

4.3. Rotor unbalance

Using the methodology described in 2.3, the vibration response to rotor unbalance was simulated for eccentricities of 0.2, 0.35 and 0.5mm. Figure 10 shows a comparison of the fast Fourier transform (FFT) of an unmodified vibration sample acquired at 2000 rpm and the FFT of the corresponding simulated rotor imbalance.

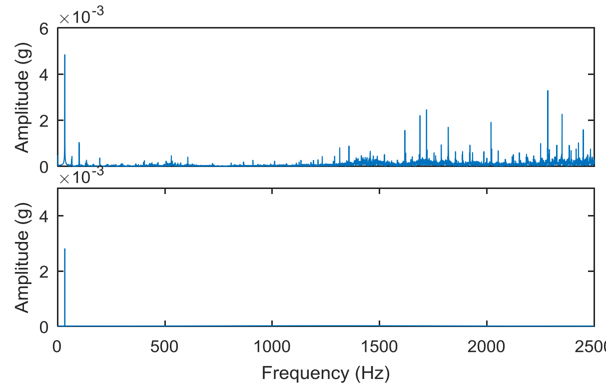

Figure 10: FFT of a vibration sample at 2000 rpm (top) and rotor unbalance with 0.5 mm of eccentricity (bottom).

The original signal is dominated in the low frequencies by the rotation speed (33.3 Hz) and its second and third harmonic, showing also relatively high levels of activity at higher frequencies in the range of 1500 to 2500 Hz. The simulated response to unbalance basically contains a sinusoidal component with the same frequency as the driving force. In the case of unbalance, the frequency and phase of the driving force were chosen to be equal to the frequency and phase of the 1X peak in each vibration sample. The amplitude of the driving force was calculated from Eq. (3) and the vibration response was obtained solving Eq. (2). Both signals, real and simulated, were then added to generate the faulty signal from which the CIs were extracted. **Table 1** shows the detection rate for each indicator and each eccentricity studied. Detection rate is calculated as the percentage of normalised CI samples providing a value higher than 1.

e	RMS	CF	K	1X	2X
0.2	11.2	15.6	16.8	88.9	12.1
0.35	19.4	18.1	15.4	92.8	12.9
0.5	35.3	21.4	17.2	100	12.7

Table 1: % Fault detection % (unbalance)

The results summarised in **Table 1** indicate that the only CI providing a clear indication of the presence of the fault was the amplitude of the peak at 1X in the frequency domain. The detection rate was significantly high (88.9 %) even for the first case studied (0.2 mm), achieving a 100% detection rate in the most severe case (0.5 mm). Despite the normalization process, the behaviour of the indicator showed some dependency on the rotational speed that hindered detection at low speeds with low fault severity. This is attributed to the fact that the fault injected depends on the square of the speed (see Eq. (3)) and hence its influence at low speeds is much smaller than at high speeds. General indicators from the time domain (RMS, CF and K) showed a poor detection performance. RMS increased slightly as the fault progressed, indicating a small increment in the energy of the signal (especially at high speeds). CF and K showed almost no variation, which is understandable as they are designed to detect impulse-like events. The amplitude of the peak at 2X did not show any significant changes as this frequency component of the signal was not affected by the fault injected.

4.4. Gear fault

The vibration response of a virtual gear with a damaged tooth was simulated using the method described in 2.3. Assuming a gearbox with perfect meshing (not producing vibration at the gear mesh frequency) the additional forces generated by one tooth with a damaged meshing surface were simulated as a series of impacts happening once per revolution. For simplicity the impact duration was set to 20% of the time between two consecutive teeth meshing, and the force amplitude was constant for all the regimes tested in each case. Three different severity cases were studied, using impact amplitudes of 100, 500 and 1000 N. Figure 11 shows the FFT of a simulated tooth surface fault signal at 2000 rpm.

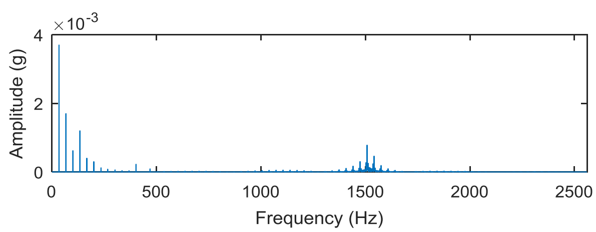

Figure 11: FFT of tooth surface fault at 2000 rpm (1000 N)

In this case the simulated response to a sequence of impacts is dominated by the rotating speed frequency (around 33.3 Hz) and its harmonics, as well as some activity around the natural frequency (1517 Hz). Table 3 shows the detection rate for each indicator and each load studied.

Case	RMS	CF	K	1X	2X
100 N	11.6	15.4	31.2	65.2	57.4
500 N	24.1	22.6	52.8	82.1	71.6
1000 N	51.3	31.2	65.7	92.7	84.9

Table 2: % Fault detection % (gear fault).

The results summarised in Table 3 indicate that the most sensitive CI for this fault was again the amplitude of the frequency peak at the rotating frequency (1X). The second harmonic of the rotating speed (2X) also shows a very good sensitivity in this case, due to the harmonics produced by the response to the impacts. Kurtosis was also successful in the later stages of degradation, reaching 65.7 % detection rate for the 1000 N case. RMS showed a noticeable increment in the 500 N and 1000N cases, but the detection rate just reached 51.3% in the best case. Crest factor showed just a slight increment, probably due to the fact that the maximum signal amplitude is normalised by the signal RMS which also increased, hindering the performance of this indicator.

5. CONCLUSION

This study presented a novel vibration-based technique for rotorcraft gearbox monitoring under varying operating conditions. This technique is based on the extraction of key indicators and the generation of indicator maps for any operating condition tested based on the statistical analysis of clustered observations. The objective of these maps is to define a baseline for the value of the indicators for a range of operating conditions in the absence of faults. Normalization of the CIs using these baseline maps minimizes their dependency on the operating conditions and allows direct comparison of all the CIs with a common threshold for fault detection.

The performance of the proposed method was tested using vibration data acquired from a compressor rig operating at different regimes. Initially the CI normalization procedure was validated using a data set which included conditions not seen in the training data set used to construct the maps. The results showed that normalization based on interpolation of these maps minimises the dependency of the indicators on operating conditions. Two mechanical faults with different characteristics were seeded into the data simulating the vibration response of these faults. The results showed that condition indicators specifically chosen for the detection of these particular faults, such as specific peaks in the FFT, are highly sensitive to the changes produced in the signal. These indicators provided very high detection rates for the whole range of operating conditions used during the test. Other condition indicators that characterise the signal globally were not so successful, and only provided high detection rates when the simulated degradation was high.

These results prove the importance of the selection of appropriate condition indicators for the faults expected in the system. The inclusion of specific indicators that are sensitive to faults and provide information about their origin is key even under stationary operation. The application of the proposed mapping and normalization approach allows the operator to assess the condition of the system in a wide variety of conditions, making it suitable for its application in rotorcraft gearboxes or any other mechanical system working at different operating regimes.

ACKNOWLEDGEMENT

The iGear project has received funding from the Clean Sky 2 Joint Undertaking under the European Union's Horizon 2020 research and innovation programme under grant agreement No 738144.

The data used in this publication was produced with the financial support from the Marie Curie FP7-ITN project "ENERGY-SMARTOPS", Contract No: PITN-GA-2010-264940.

REFERENCES

Bartelmus, W., & Zimroz, R. (2009). Vibration condition monitoring of planetary gearbox under varying external load. *Mechanical Systems and Signal Processing*, *23*(1), 246–257.

Baydar, N., & Ball, A. (2001). A comparative study of acoustic and vibration signals in detection of gear failures using Wigner-Ville distribution. *Mechanical Systems and Signal Processing*, *15*(6), 1091–1107.

Kasabov, N. K., & Song, Q. (2002). DENFIS: dynamic evolving neural-fuzzy inference system and its application for time-series prediction. *Fuzzy Systems, IEEE Transactions on*, *10*(2), 144–154.

McFadden, P. D. (1986). Detecting fatigue cracks in gears by amplitude and phase demodulation of the meshing vibration. *Journal of Vibration, Acoustics, Stress, and Reliability in Design*, *108*(2), 165–170.

Morgan, N. T., Berrigan, C. S., Lopez, M. J. S., & Prasad, J. V. R. (2017). Application of Linear Quadratic Estimation to Harmonic Analysis of Rotorcraft Vibration. *Journal of Guidance, Control, and Dynamics*, *40*(9), 2348–2354.

Parker Jr., B. E., Ware, H. A., Wipf, D. P., Tompkins, W. R., Clark, B. R., Larson, E. C., & Poor, H. V. (2000). Fault diagnostics using statistical change detection in the bispectral domain. *Mechanical Systems and Signal Processing*, *14*(4), 561–570.

Ruiz-Cárcel, C., Jaramillo, V. H., Mba, D., Ottewill, J. R., & Cao, Y. (2016). Combination of process and vibration data for improved condition monitoring of industrial systems working under variable operating conditions. *Mechanical Systems and Signal Processing*, *66–67*, 699–714.

Samuel, P. D., & Pines, D. J. (2005). *A review of vibration-based techniques for helicopter transmission diagnostics*. *Journal of Sound and Vibration* (Vol. 282)

Zhan, Y., Makis, V., & Jardine, A. K. S. (2006). Adaptive state detection of gearboxes under varying load conditions based on parametric modelling. *Mechanical Systems and Signal Processing*, *20*(1), 188–221.

Zimroz, R., Bartelmus, W., Barszcz, T., & Urbanek, J. (2014). Diagnostics of bearings in presence of strong operating conditions non-stationarity—A procedure of load-dependent features processing with application to wind turbine bearings. *Mechanical Systems and Signal Processing*, *46*(1), 16–27.

BIOGRAPHIES

Dr. Cristobal Ruiz-Carcel Cristobal received his degree in mechanical engineering in 2010 from Universidad Politecnica de Valencia (Spain), followed by an MSc Eng. degree in Design of Rotating Machines from Cranfield University in 2011. In 2014 he completed his PhD in the field of condition monitoring applied to large scale industrial systems at Cranfield University, which was part of the Marie Curie FP7 project "Energy-Smartops".Cristobal's main research interests have been focused on signal processing algorithms, multivariate data analysis, condition monitoring and predictive maintenance. He is currently a Research Fellow at the Through-life Engineering Services Institute, where he is working on the development, testing, and implementation of novel monitoring techniques for different applications.

Prof. Andrew Starr is Head of the Through-life Engineering Services Institute, a world-leading centre of excellence in maintenance and asset management for high value systems. The TES Institute works in partnership with industry in research and education. Professor Starr read Mechanical Engineering at the University of Leeds, while sponsored by British Aerospace (Civil Aircraft), for which he was awarded first prize in the final year of his apprenticeship. He studied for his doctoral thesis in condition based maintenance for robotic production plant at the University of Manchester, sponsored by Ford and Wolfson Maintenance. He has held academic posts at the University of Huddersfield, the University of Manchester, and the University of Hertfordshire, as Head of the School of Aerospace, Automotive and Design Engineering. He has published over 150 technical papers from a wide range of collaborative projects with industry, helping to solve real problems and to devise innovative products and services.

Dr. James R. Ottewill received the B.Eng. degree (with honors) in mechanical engineering from the University of Bristol, Bristol, UK in 2005 and the Ph.D. degree in mechanical engineering from the same university in 2009. He is currently a Senior Principal Scientist at ABB Corporate Research Center in Kraków, Poland working in the field of applied analytics for condition monitoring applications. His main research interests relate to advanced physics-based and data-driven approaches for diagnostics and prognostics including dynamic testing, modeling and analysis of non-linear systems, signal processing and information fusion. Dr. Ottewill is a Chartered Engineer in the U.K. and a Member of the Institution of Mechanical Engineers, U.K.